Size effects on the electronic structure of ErSb nanoparticles embedded in the GaSb(001) surface

J. K. Kawasaki, B. D. Schultz, and C. J. Palmstrøm

Phys. Rev. B **87**, 035419 — Published 22 January 2013

DOI: 10.1103/PhysRevB.87.035419

Size Effects on the Electronic Structure of ErSb Nanoparticles Embedded in the GaSb(001) Surface

J. K. Kawasaki,[1] B. D. Schultz,[2] and C. J. Palmstrøm[1,2]

[1]Materials Department
[2]Department of Electrical & Computer Engineering
University of California, Santa Barbara, CA 93106

ABSTRACT

The dependence of the electronic structure of ErSb nanoparticles embedded in GaSb(001) surfaces on particle size is investigated by *in-situ* scanning tunneling microscopy and spectroscopy. By varying growth conditions, the planar dimensions and surface termination of ErSb nanoparticles can be controlled. As the deposition temperature is raised, ErSb nanoparticles become increasingly elongated along the <-110> directions due to anisotropic surface diffusion. The local density of states is measured by tunneling point spectroscopy. ErSb nanoparticles were found to be semimetallic with no discernible band gap, despite predictions from finite potential quantum confinement calculations that suggest the smallest particles should become semiconducting.

Controlling the electronic properties and atomic scale growth mechanisms of confined structures is critical to the design of nanoscale optical and electronic devices. One promising nanocomposite system consists of rare-earth monopnictide (RE-V) nanostructures embedded within a III-V semiconducting matrix. This system has already shown a range of functionalities, such as enhanced interband tunneling across p-n junctions [1,2], spin-dependent resonant tunneling [3,4], fast electron-hole recombination for THz devices [5], both electrical doping and phonon scattering for thermoelectrics [6,7], and giant magnetoresistance [8,9].

However, the electronic structure of RE-V compounds in confined geometries remains unclear [10–15]. While bulk Er-monopnictides ErP, ErAs, and ErSb are semimetals with Γ-X band overlap [16–18], basic quantum confinement models predict the opening of a band gap for ErAs thin films with thicknesses below 1.7 nm [11,19] and for ErAs nanoparticles with diameters less than 3 nm [12]. However, cross-sectional scanning tunneling spectroscopy measurements for ErAs nanoparticles showed no evidence of a gap, suggesting that simple hard-walled potential models are not sufficient to describe confined ErAs/GaAs structures [10,15]. Tunneling point spectroscopy measurements of ErP nanoparticles on InP(001) surfaces [13] suggest a gap opening may occur in ErP nanoparticles; however, the samples were exposed to air prior to the measurements and Er-based compounds are known to oxidize rapidly [20,21]. Similar tunneling spectroscopy results have also been reported for Er precipitates in bulk GaSb crystals following their exposure to air [14]. Whether the ErP and ErSb nanoparticles become semiconducting from quantum confinement or due to oxidation is still to be determined.

ErSb nucleates on the GaSb(001) surface via an embedded growth mode where impinging Er atoms displace Ga from the zincblende GaSb surface and bond with the remaining Sb to form rocksalt ErSb nanoparticles [6 ,7]. The nanoparticles extend three to four atomic layers into the surface, and their depth is limited by the low diffusivity of Er through ErSb. The displaced Ga atoms are free to move on the surface and bond with the impinging Sb_2 flux to re-grow GaSb. Based on this growth mechanism, changes in growth temperature should impact the surface mobilities of the Er and Ga atoms and produce variations in the structural, electronic and magnetic properties of the resulting nanocomposite. The nanoparticle size dependence and spatial distribution also impact the magneto dependent hopping transport by altering the size and distribution of the bound magnetic polarons in these nanocomposites [8,9].

In this letter, scanning tunneling microscopy (STM) and spectroscopy (STS) are used to investigate the influence of substrate temperature on the growth of ErSb nanoparticles on GaSb(001) surfaces and to measure the effect of quantum confinement on the electronic structure of ErSb nanoparticles.

Samples were grown on GaAs(001) epi-ready substrates by molecular beam epitaxy in a modified VG V80H system with a base pressure $<5\times10^{-11}$ mbar. After thermal desorption of the surface oxide under an As overpressure, a 200 nm GaAs buffer layer was grown at 540 °C, followed by a 200 nm GaSb layer at 500 °C. Both layers were doped with 1×10^{18} Si atoms/cm^3. The sample temperature was then ramped to the desired growth temperature for ErSb (between 400 – 540 °C) and annealed with an Sb overpressure sufficient to maintain a strong $c(2\times6)$ reconstruction as observed by reflection high-energy electron diffraction (RHEED). For growth temperatures below 430°C the Sb overpressure was reduced to prevent a transition to the $c(2\times10)$ reconstruction, and for growth temperatures above 530°C the Sb overpressure was increased to prevent decomposition of the surface. Er was then codeposited with the Sb using a high temperature effusion cell to produce a 0.6 monolayer (ML) equivalent coverage of ErSb, where 1 ML is defined to contain 5.4×10^{14} Er atoms/cm^2 and 5.4×10^{14} Sb atoms/cm^2. Deposition rates

were calibrated from Rutherford backscattering spectrometry measurements (RBS) and from RHEED intensity oscillations obtained from ErAs growth on GaAs(001) surfaces. Following the growth of 0.6 ML ErSb, both the Er and Sb sources were shuttered and the sample was rapidly quenched to room temperature to retain the *c*(2×6) reconstruction. Sample temperatures were measured using a pyrometer and a thermocouple in contact with the sample block. After growth, samples were transferred *in-situ* through ultrahigh vacuum ($<1\times10^{10}$ mbar) to an Omicron variable temperature scanning tunneling microscope (VT-STM) to avoid sample contamination and oxidation. STM and STS were performed at room temperature.

Figure 1 shows a series of STM images for 0.6 ML ErSb on GaSb(001) grown at temperatures ranging from 400 to 540°C. The ordered rows of Sb dimers oriented along [-110] correspond to the *c*(2×6) surface reconstruction of GaSb(001). Figure 1(c) shows ErSb nanoparticles nucleated at 500°C. Two different types of ErSb nanoparticles are identified as previously reported [22]. Type A nanoparticles have their top most surface rising one atomic layer (3 Å) above the GaSb surface and type B particles have their top most surface in plane with the GaSb surface. The latter type B particles result from step-flow GaSb re-growth arising from the Er-Ga displacement reaction around type A particles.

The ErSb nanoparticles in Figure 1(c) are clearly distinguishable from the GaSb matrix as they do not exhibit the *c*(2×6) reconstruction of the GaSb. Instead, the ErSb particles are terminated with a mixture of rectangular domains oriented along the [110] and [-110] directions as shown in the Figure 1(c) inset. The lateral spacings are consistent with the (1×4)/(4×1) pattern observed previously for ErSb films by low energy electron diffraction (LEED) and RHEED [22,24,25]. This mixed phase reconstruction has been attributed to a sub-monolayer coverage of GaSb that rides on the surface of the ErSb as a result of the Er-Ga displacement mechanism [22]. The (1×4)/(4×1) ErSb regions account for ~15% of the sample surface, consistent with the surface coverage expected for the deposition of 0.6 ML ErSb nanoparticles with an average thickness of 4 atomic layers.

For growth at 540°C [Figure 1(d)], both type A and B particles are again identified and the surfaces show a mixed domain reconstruction, however the reconstruction is more disordered than for growth at 500°C. Additionally there are small clusters on the surface, which could be small ErSb particles or clusters of GaSb. The disorder in the large ErSb nanoparticles and smaller clusters may result from an increase in the desorption rate of Sb at elevated growth temperatures, which becomes comparable to the incoming Sb flux at 540°C and eventually leads to the decomposition of the GaSb surface at higher temperatures.

At a growth temperature of 450°C [Figure 1(b)], both type A and B ErSb particles are present, however, these nanoparticles are terminated with a clear (1×1) surface periodicity, as expected for an unreconstructed rocksalt ErSb surface. The (1×1) surface periodicity has also been observed by LEED and STM for ErAs(001) thin films grown at 350 ºC [25,26]. A 1.2 nm border region surrounds the edge of each ErSb nanoparticle that does not share the (1×1) surface periodicity and has similar contrast to the adjacent GaSb step edges. This border is not observed at the higher growth temperatures and is consistent with re-grown GaSb from the displaced Ga atoms. The difference suggests that an activation barrier prevents continued GaSb step-flow re-growth around the ErSb nanoparticles beyond the thin border region. The presence of type B nanoparticles indicates Ga is still able to diffuse across the GaSb surface and re-grow at the step edges as seen for higher temperatures.

When ErSb is grown at 400 °C [Figure 1(a)] the GaSb surface begins to roughen and in-plane (type B) ErSb nanoparticles are no longer observed. The type A islands still form as

square 3×3 nm nanoparticles. These square sites account for 15% of the surface, consistent with the coverage expected for 0.6 ML ErSb. The surface roughness made it difficult to achieve adequate resolution in the STM to image the atomic periodicity on the type A surfaces. In addition to type A ErSb islands, another type of surface island is found consisting of elongated strips along the [-110] that rise ~3 Å above the surface. These elongated islands are terminated with Sb dimer rows along the [-110] and are likely re-grown GaSb islands resulting from displaced Ga. The height corresponds to one atomic bilayer (3Å) of GaSb and the lateral dimension along the [110] is 2.5 nm or the width of two adjacent Sb dimer rows in the *c*(2×6) reconstruction. These elongated islands account for 50-60% of the sample surface, consistent with the amount of Ga that would be displaced by 0.6 ML ErSb. The displaced Ga atoms do not have sufficient mobility at 400 °C to diffuse to the GaSb step edges, and instead they begin to nucleate GaSb islands near the sites where they were initially displaced. There is clearly some surface diffusion as seen by the preferential elongation of the GaSb islands along the [-110].

The switch from step-flow growth to layer-by-layer growth produces the apparent roughening of the GaSb and explains why no type B (in-plane) ErSb islands are observed as they result from GaSb step-flow re-growth around type A islands [22]. For ErSb nucleation at temperatures of 500 and 540°C, the displaced Ga atoms have sufficient mobility to diffuse to step edges and particle edges and thus no GaSb islands are nucleated under stable growth conditions. The step-flow re-growth for temperatures ≥500°C is consistent with the step-flow regime observed for GaSb homoepitaxy on vicinal surfaces [27]. Growth at 450°C is an intermediate regime where some displaced Ga re-grows elongated GaSb islands on the surface [Figure 1(b)] and some re-grows GaSb around the type A ErSb nanoparticles and at GaSb step edges.

Higher growth temperatures also increase the ErSb nanoparticle sizes. As the growth temperature is raised from 400 to 540 °C, the size of the ErSb nanoparticles increase from squares with averaged in-plane dimensions of 3 nm × 3 nm to elongated rectangles with average dimensions of 8 nm × 17 nm [Figure 1(e)]. This elongation occurs preferentially along the [-110] direction due to increasing anisotropic surface diffusion of both Er and Ga adatoms along the Sb dimer rows at higher growth temperatures. This direction is also consistent with the preferential diffusion of Ga adatoms on GaAs(001) (2×4)/*c*(2×8) surfaces[22]. In the low temperature regime, the nanoparticle dimensions asymptote to an averaged minimum length of 3 nm along both <110> directions. The 3 nm length corresponds to slightly greater than the width of 2 Sb dimer rows for the GaSb *c*(2×6) reconstruction (one unit cell length along the [110] direction). This distance appears to be the minimum in-plane nucleation size for ErSb nanoparticles on the GaSb(001) *c*(2×6) surface. Despite the increase in the planar dimensions of the ErSb nanoparticles with temperature, the surface coverage of the nanoparticles in Figures 1(a-d) remains constant at roughly 15% indicating the ErSb nanoparticles maintain a thickness of 4 ML (1.2 nm) for each of the growth temperatures [Figure 1(f)].

Figure 2 shows STM tip height profiles along [110] for a single type B particle grown at 500 ºC at various sample bias voltages. The apparent height of the ErSb particle relative to the GaSb matrix varies as a function of the bias voltage, ranging from 0.2 Å above the GaSb surface at -2.0 V sample bias to 0.2 Å below the surface at +2.0 V sample bias. The bias dependence reveals the apparent height differences results from electronic rather than topographical contrast. This electronic contrast, in addition to the difference in surface reconstructions, can be used to further distinguish the ErSb nanoparticles from the GaSb matrix. The direction of change in tip height suggests that relative to the GaSb matrix, the ErSb particles have a larger valence band

density of states (filled states, resulting from tunneling of electrons from the sample to the tip at negative sample bias) and a smaller conduction band density of states (empty states, resulting from electrons tunneling from tip to sample at positive sample bias).

For a more complete measurement of the band structure, STS point spectra were also measured for nanoparticles of various in-plane dimensions. Figure 3 shows tunneling current point spectra *I(V)* for ErSb nanoparticles grown at 540, 500, and 450 °C and for the surrounding GaSb matrix. These temperatures correspond to ErSb nanoparticles with average in-plane dimensions of 8.0 nm ×17 nm, 5.3 nm×7.0 nm, and 3.3 nm ×3.3 nm, with a constant out-of-plane depth of 4 atomic layers (1.2 nm). Each spectrum was averaged over 15-20 individual nanoparticles or locations within the GaSb matrix. The STS spectra from the surrounding GaSb (bottom curve), contains a region extending from approximately -0.3 V to +0.3 V with zero tunneling current consistent with the expected band gap of GaSb. The Fermi level (V=0) is found to be mid-gap, in contrast with the p-type character expected for Si-doped GaSb [29]. The mid-gap position is likely a result of surface Fermi level pinning.

For the largest ErSb particles grown at 540 °C there is a clear overlap between valence and conduction bands with no discernible band gap, which is consistent with semimetallic ErSb in the bulk limit. For the smaller particles, both those grown at 500 °C and those at 450 °C, simple quantum confinement models predict a gap should start to open [11,12]. Despite these predictions, STS measurements show there are still overlapping valence and conduction bands and no sign of a band gap opening. The ErSb nanoparticles remain semimetallic down to the smallest particles (3.3 nm×3.3 nm) that could be nucleated on GaSb. This is consistent with previous studies in the ErAs/GaAs system, where ErAs nanoparticles were also found to be semimetallic [10,15]. These metal/semiconductor interfaces play an important role in plasmonics [30]. The ability to grow very small metallic nanoparticles embedded within a semiconducting matrix extends the range of accessible plasmon frequencies, and the ability to control the anisotropy of the particles via growth enables tuneablity of multiple plasmon modes.

In addition to the lateral dimensions of the ErSb nanoparticles, the surface termination may be expected to affect the nanoparticle local density states (LDOS). As noted earlier, for growth at 500°C and higher the (1×4)/(4×1) surface termination of the ErSb nanoparticles has been attributed to a sub-monolayer coverage of Ga that rides on top of the ErSb nanoparticles [Figure 1(c) inset], whereas a (1×1) surface periodicity is observed for Ga-free ErSb surfaces [Figure 1(b) inset]. The bonding of the residual Ga on the ErSb surface is not known, and from the STS spectra the effect of residual Ga on the nanoparticle LDOS remains unclear. Further photoemission and low temperature STS studies may help to elucidate the effect of Ga-termination on the ErSb surface.

In summary, ErSb nucleates on GaSb(001) surfaces via an embedded growth mode, which is strongly dependent on growth temperature. At high growth temperatures, the high surface mobility of both Er and Ga adatoms leads to elongated nanoparticles with a Ga-induced (1×4)/(4×1) surface reconstruction, and the surrounding GaSb matrix remains smooth due to the step-flow re-growth of the displaced Ga. At low temperatures, the reduced surface mobility of Er and Ga adatoms leads to smaller square ErSb nanoparticles with a (1×1) surface periodicity, and the surrounding GaSb matrix roughens due to predominantly layer-by-layer re-growth of GaSb islands. The smallest ErSb nanoparticles that could be nucleated measured 3.3 nm×3.3 nm in size and approximately 1.2 nm in height. In-situ STS measurements showed that no band gap formed in any of the ErSb nanoparticles nucleated, indicating the particles remain semimetallic even at sizes below where quantum confinement is expected to open a gap. This preserved metallicity, in

addition to control of the nanoparticle size, anisotropy, and surface termination, enables the design of highly tunable plasmonics, metamaterials, spintronics, and other "active metal" devices.

The authors thank A.C. Gossard for fruitful discussions. This work was supported in part by funding from the NSF-MRSEC (grant number DMR-1121053) and the AFOSR (grant number FA9550-10-1-0119). J. K. acknowledges funding from the NDSEG Fellowship.

[1] J. M. O. Zide, A. Kleiman-Shwarsctein, N. C. Strandwitz, J. D. Zimmerman, T. Steenblock-Smith, A. C. Gossard, A. Forman, A. Ivanovskaya, and G. D. Stucky, Appl. Phys. Lett. **88**, 162103 (2006).

[2] H. P. Nair, A. M. Crook, and S. R. Bank, Appl. Phys. Lett. **96**, 222104 (2010).

[3] D. E. Brehmer, K. Zhang, C. J. Schwarz, S.-P. Chau, S. J. Allen, J. P. Ibbetson, J. P. Zhang, C. J. Palmstrøm, and B. Wilkens, Applied Physics Letters **67**, 1268 (1995).

[4] A. G. Petukhov, W. R. L. Lambrecht, and B. Segall, Phys. Rev. B. **53**, 3646–3649 (1996).

[5] M. P. Hanson, D. C. Driscoll, J. D. Zimmerman, A. C. Gossard, and E. R. Brown, Appl. Phys. Lett. **85**, 3110 (2004).

[6] J. Zide, D. Vashaee, Z. Bian, G. Zeng, J. Bowers, a. Shakouri, and a. Gossard, Physical Review B **74**, 1–5 (2006).

[7] J. M. Zide, D. O. Klenov, S. Stemmer, a. C. Gossard, G. Zeng, J. E. Bowers, D. Vashaee, and a. Shakouri, Applied Physics Letters **87**, 112102 (2005).

[8] D. Schmidt, A. G. Petukhov, M. Foygel, J. P. Ibbetson, and S. J. Allen, Phys. Rev. Lett. **82**, 823–826 (1999).

[9] A. G. Petukhov and M. Foygel, Phys. Rev. B. **62**, 520–531 (2000).

[10] J. K. Kawasaki, R. Timm, T. E. Buehl, E. Lundgren, A. Mikkelsen, A. C. Gossard, and C. J. Palmstrøm, J. Vac. Sci. Tech. B. **29**, 03C104 (2011).

[11] S. J. Allen, N. Tabatabaie, C. J. Palmstrøm, S. Mounier, G. W. Hull, T. Sands, F. DeRosa, H. L. Gilchrist, and K. C. Garrison, Surf. Sci. **228**, 13–15 (1990).

[12] M. A. Scarpulla, J. M. O. Zide, J. M. LeBeau, C. G. Van De Walle, A. C. Gossard, and K. T. Delaney, Appl. Phys. Lett. **92**, 173116 (2008).

[13] L. Bolotov, T. Tsuchiya, A. Nakamura, T. Ito, Y. Fujiwara, and Y. Takeda, Phys. Rev. B. **59**, 12236–12239 (1999).

[14] P. Hidalgo, B. Méndez, J. Piqueras, J. Plaza, and E. Diéguez, J. Appl. Phys. **86**, 1449 (1999).

[15] J. K. Kawasaki, R. Timm, K. Delaney, E. Lundgren, A. Mikkelsen, and C. J. Palmstrøm, Phys. Rev. Lett. **107**, 036806 (2011).

[16] R. Bogaerts, F. Herlach, De Keyser A., F. M. Peeters, F. DeRosa, C. J. Palmstrøm, D. Brehmer, and S. J. Allen, Phys. Rev. B. **53**, 15951–15963 (1996).

[17] A. G. Petukhov, W. R. L. Lambrecht, and B. Segall, Phys. Rev. B. **53**, 4324–4339 (1996).

[18] L. Pourovskii, K. T. Delaney, C. G. Van de Walle, N. Spaldin, and A. Georges, Phys. Rev. Lett. **102**, 2–5 (2009).

[19] V. Sandomirskii, Soviet Journal of Experimental and Theoretical Physics **25**, 101 (1967).

[20] L. Murr, Physica Status Solidi (b) **135**, (1967).

[21] S. Kennou, S. Ladas, M. G. Grimaldi, T. A. Nguyen Tan, and J. Y. Veuillen, Appl. Surf. Sci. **102**, 142–146 (1996).

[22] B. D. Schultz, S. G. Choi, and C. J. Palmstrøm, Appl. Phys. Lett. **88**, 243117 (2006).

[23] B. D. Schultz and C. J. Palmstrøm, Phys. Rev. B. **73**, 1 (2006).

[24] A. Guivarch, Y. Ballini, Y. Toudic, M. Minier, P. Auvray, B. Guenais, J. Caulet, B. Le Merdy, B. Lambert, and A. Regreny, J. Appl. Phys. **75**, 2876 (1994).

[25] B. D. Schultz, Ph.D. Thesis, Univ. Minnesota (2006).

[26] T. Komesu, H.-K. Jeong, J. Choi, C. Borca, P. Dowben, A. Petukhov, B. D. Schultz, and C. J. Palmstrøm, Phys. Rev. B. **67**, (2003).

[27] N. Bertru, M. Nouaoura, and J. Bonnet, J. Cryst. Growth **160**, 1–6 (1996).

[28] K. Shiraishi, Appl. Phys. Lett. **60**, 1363–1365 (1992).

[29] T. M. Rossi, D. A. Collins, D. H. Chow, and T. C. McGill, Appl. Phys. Lett. **57**, 2256–2258 (1990).

[30] E. Brown, A. Bacher, D. Driscoll, M. P. Hanson, C. Kadow, and A. C. Gossard, Phys. Rev. Lett. **90**, 17–20 (2003).

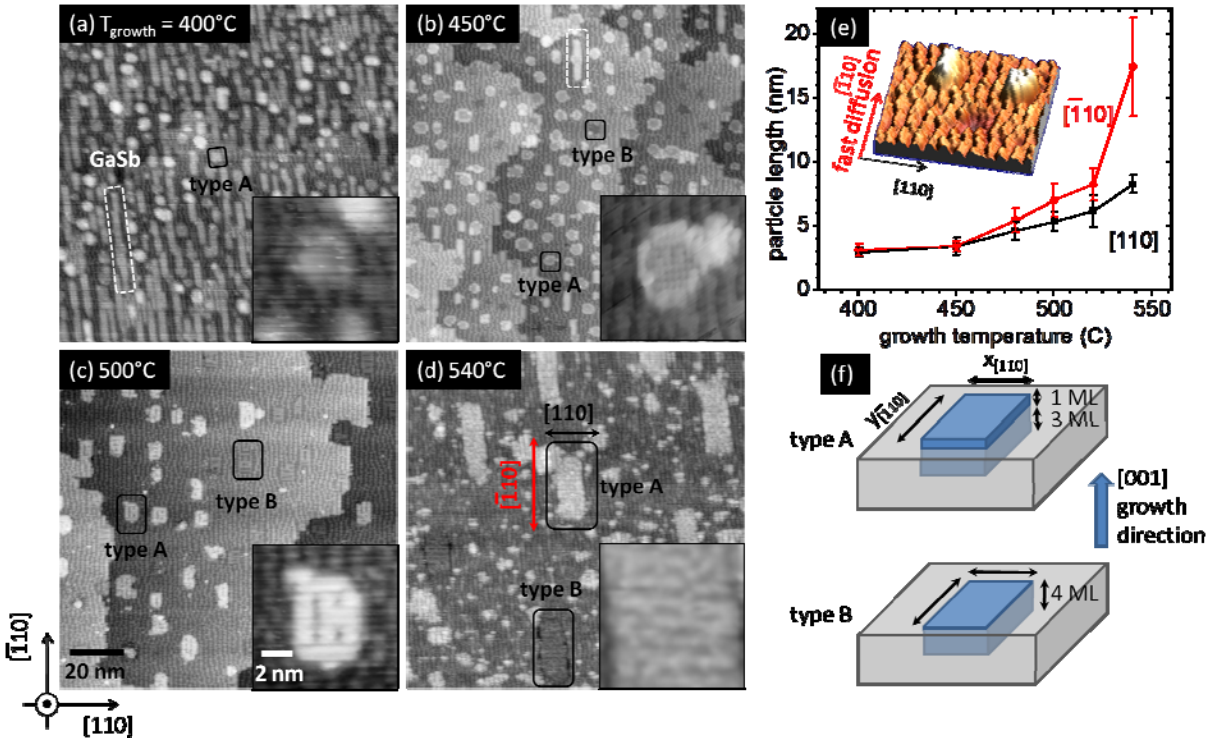

Figure 1. (a-d) 100×100 nm STM images of 0.6 ML ErSb nucleated on the GaSb(001) surface at various growth temperatures. Insets: 6 nm×6 nm images showing the ErSb nanoparticle surface reconstructions. (e) Average ErSb nanoparticle dimensions along [-110] and [110] as a function of growth temperature. (f) Schematic of type A and B ErSb nanoparticles.

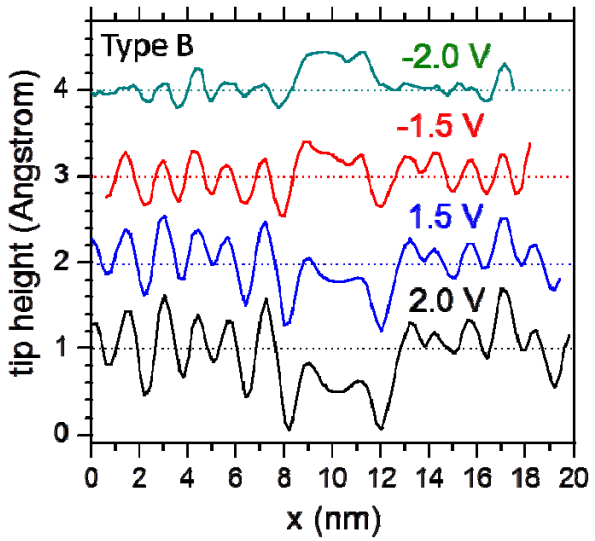

Figure 2. Tip height profiles along [110] for a single type B ErSb nanoparticle (top surface resides in-plane with the GaSb) at various sample bias voltages, demonstrating that the ErSb is electronically distinguishable from the GaSb matrix. The particle was nucleated at 500°C.

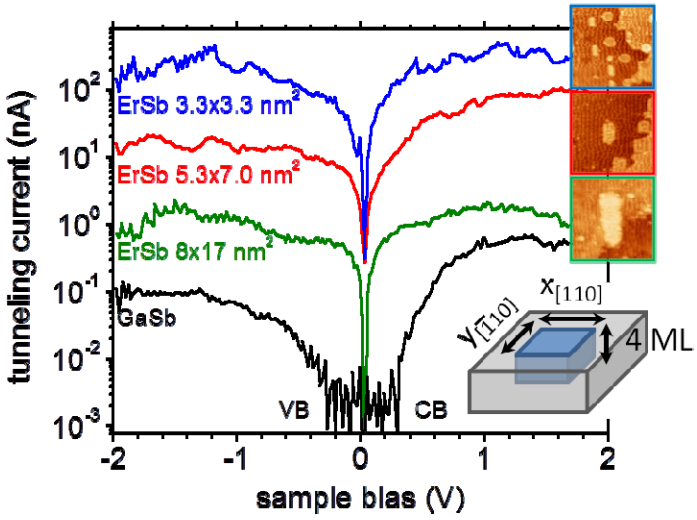

Figure 3. Tunneling *I(V)* point spectra for the GaSb matrix and for ErSb nanoparticles with in-plane dimensions of 3.3 nm×3.3 nm, 5.3 nm×7.0 nm, and 8.0 nm×17 nm and a constant thickness of 4 atomic layers (1.2 nm) These dimensions correspond to growth temperatures of 450, 500, and 540 °C respectively.